3rd URSI AT-AP-RASC, Gran Canaria, 29 May – 3 June 2022

On the Impact of Transfer Impedance and Grounding on RF Measurement Results

Carlo Carobbi, Lorenzo Capineri, and Leonardo Vignoli
University of Florence, Dep. of Information Engineering, 50139, Firenze, Italy

Abstract

The impact of the transfer impedance of single-ended connections on the reliability of measurement results and the need for appropriate grounding are highlighted through an application in electromagnetic compatibility testing. A review about transfer impedance and its role in the generation of an undesired common mode voltage is provided.

1. Introduction

The transfer impedance of coaxial cables and shielded cable assemblies is a well-known quantity in the field of electromagnetic compatibility (EMC) and radiofrequency (RF) measurements. Standards are available defining the transfer impedance and measurement methods covering a relatively large frequency bandwidth [1]. The uncertainty of transfer impedance measurement has been investigated [2-3]. Research is still ongoing to simplify and improve transfer impedance measurement methods (see [4]). A review on transfer impedance of shielded cables and its measurement methods is available in [5-7].

The concept of transfer impedance can be extended from coaxial and shielded cable assemblies to any sort of single-ended (ground referenced or unbalanced) connection, such as a trace over a metallic ground plane in a printed circuit board (PCB). The reason why a PCB with attached cables generates radiated electromagnetic interference (EMI) is the imperfect magnetic field shielding offered by the finite size PCB reference plane, as clarified in the seminal work [8]. The so called "common mode inductance" constitutes the transfer impedance of the trace-reference plane assembly.

The scope here is to highlight the role of transfer impedance in determining the quality of EMC and RF measurement results. In particular, due to the non-zero transfer impedance of single-ended connections, it is demonstrated that a common-mode voltage arises that, in specific situations, may adversely impact measurement results. Appropriate grounding can alleviate this adverse effect at the expense of a remarkable common mode current. The work is in the vein of others devoted to improvement of the quality of EMC and RF measurements and to reduction of measurement and system modelling uncertainty [9-10].

In the next section 2 the definition of transfer impedance is recalled. The effect of transfer impedance on RF voltage measurements is analyzed and quantified through simple circuit modelling in section 3. An application to EMC measurement is illustrated in section 4.

2. Transfer Impedance

Consider a single ended connection between a source and a load consisting of conductors S and G, where S is the signal conductor and G is the ground conductor. Conductor G is grounded to a third conductor represented by a Reference Ground Plane (RGP), see Figure 1. We assume that the RGP is perfectly conducting and of infinite size. The length of the single ended connection is l, which is short with respect to wavelength, so that the lumped circuit model approximation is valid.

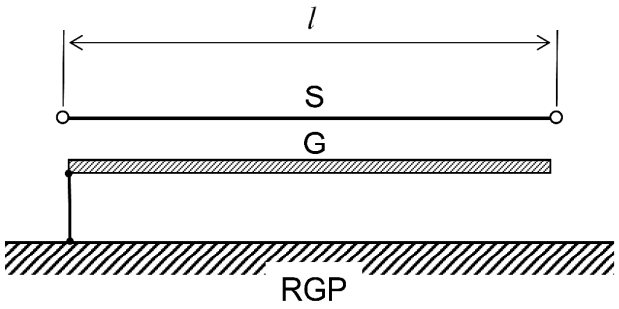

Figure 1. A single-ended connection between a source and a load (source and load not represented) over a reference ground plane.

A current source is now connected between G and RGP at the right side, a voltmeter is connected between S and G at the left side and a short circuit is connected between S and G at the right side, see Figure 2. The transfer impedance Z_T is defined as

$$Z_T = \frac{V}{I} \cdot \frac{1}{l}, \tag{1}$$

where I is the injected current and V is the voltage measured by the voltmeter. By definition, Z_T is a per-unit-length parameter.

Consider now the case where the positions of the current source and of the voltmeter are swapped, see Figure 3. By reciprocity, we have that if the same current I is injected between S and G at the left side, then the same voltage V is measured between G and RGP at the right side, according to (1).

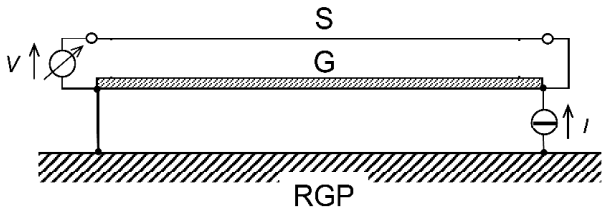

Figure 2. A current flowing through conductor G and on the RGP induces a voltage between conductors S and G.

To summarize, if a current I is injected in the G conductor a voltage V is developed between the S and G conductors. If the same current I is injected between S and G conductors a voltage V is developed between conductors G and RGP. These effects can be interpreted by attributing an impedance $Z_T \cdot l$ to the conductor G, across which a longitudinal voltage V is developed by the flow of current I.

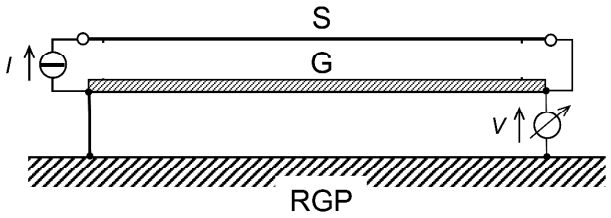

Figure 3. A current flowing through conductors S and G induces a voltage between conductors G and the RGP.

3. Load Voltage Measurement

Let us now consider the case where a source drives the single-ended connection and a load impedance Z_L is connected at the right side, see Figure 4.

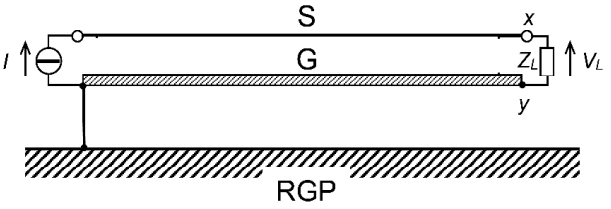

Figure 4. Measurement of the voltage V_L across load impedance Z_L as difference between RGP-referenced voltages V_x and V_y.

The current flowing through Z_L is I and suppose that the voltage V_L across Z_L is to be measured. We name x and y the terminals at which impedance Z_L is connected to conductors S and G, respectively. Let V_x and V_y be the voltages between these nodes and the RGP. Then the differential voltage across Z_L (or "differential mode" voltage) is

$$V_L = V_x - V_y = Z_L \cdot I\,, \tag{2}$$

and the common voltage to nodes x and y (or "common mode" voltage) is

$$V_y = Z_T \cdot l \cdot I\,. \tag{3}$$

To minimally perturb the circuit under measurement the voltmeter used to measure voltage V_L should be floating, otherwise, if the voltmeter was grounded to the RGP, a common mode current would flow on the RGP that does not exist in the circuit prior to the connection of the voltmeter. Further, the voltmeter should have sufficient common mode rejection, CMR, to properly measure V_L on top of V_y. It should be

$$CMR >> \frac{|Z_T| \cdot l}{|Z_L|}\,. \tag{4}$$

The worst-case situation is the one where $|Z_T|$ is large, the single-ended connection is long and $|Z_L|$ is small.

When inequality (4) cannot be met because $|V_y|$ is relatively large with respect to $|V_L|$ then, a possible solution is to tie node y to the RGB. As anticipated, this connection affects the currents in the circuit, in that a common mode current will flow on the RGP. To focus on this effect, we need to get some more physical insight into the transfer impedance.

We then consider the circuit model sketched in Figure 5, where R_S and L_S represent the resistance and self-inductance of conductor S, R_G and L_G represent the resistance and self-inductance of conductor G and M represents the mutual inductance between the meshes formed by each conductor and the RGP. Two cases are now considered, the one where node y is floating, the other where node y is connected to the RGP.

Through straightforward circuit analysis we obtain the following results. If y is floating, then $I = I_S = I_G$ and

$$\frac{V_y}{I} = R_G + j\omega\left(L_G - M\right). \tag{5}$$

Due to (1) we have

$$Z_T \cdot l = R_G + j\omega\left(L_G - M\right). \tag{6}$$

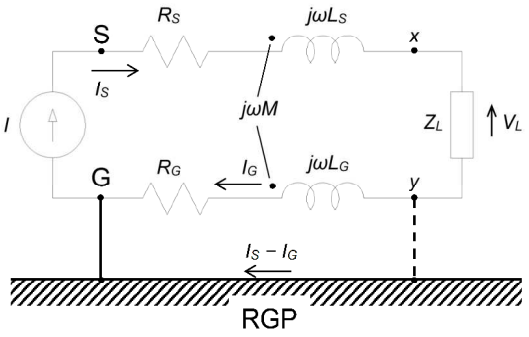

Figure 5. Equivalent circuit model of the single-ended connection formed by conductors S and G over the RGP.

We see from (6) that Z_T can be interpreted as the combination of two terms: R_G, which represents ohmic losses of conductor G, and $L_G - M$ which represents the residual magnetic flux through the mesh formed by conductor G and the RGP. Ideally, $R_G = 0$ and $L_G = M$ if G were, for example, a flat perfect electric conductor of infinite extent, or surrounding S. If y is tied to the RGP then we obtain

$$\frac{I_G}{I_S} = \frac{j\omega M}{R_G + j\omega L_G}. \quad (7)$$

Note from (7) that, at DC, $I_G = 0$, so current I_S returns to the source through the RGP. $|I_G|$ increases at increasing frequency from DC, and tends to $M/L_G \cdot |I_S| < |I_S|$ for frequency $f \gg f_G$, where

$$f_G = \frac{R_G}{2\pi L_G}. \quad (8)$$

(8) can be easily interpreted considering that the path for current return is the minimum impedance one. Thus, the path followed by current is the minimum resistance one (i.e., through the ideal RGP) for frequency below f_G, and the minimum inductance one (i.e., through conductor G) for frequency above f_G. Frequency f_G depends on electrical properties of the conductor G and it is usually of the order of a few kilohertz. For example, in the case of $l = 1$ m of RG 58 C/U cable at 5 cm above the RGP we have $L_G = 0.82$ μH. The shield resistance is $R_G = 11$ mΩ, then $f_G = 2.2$ kHz. At frequencies well above f_G a residual common mode current $I_S - I_G$ flows on the RGP. The common mode current cannot be predicted since it depends on the a-priori unknown ratio M/L_G but it can be measured by using a current probe to quantify the perturbation effect due to the connection to the RGP of node y.

4. Application

As an application of the concepts illustrated in the previous two sections consider an electromagnetic compatibility test in which a sinusoidal signal is coupled to the power supply of a printed circuit board (PCB) to evaluate electronics immunity to disturbances in the frequency range from 10 kHz to 5 MHz (immunity is evaluated through the bit-error-rate of a transceiver module, not presented here). The structure of the experimental setup is sketched through the block diagram in Figure 6. An Arbitrary Waveform Generator (AWG) feeds a Power Amplifier (PA) that generates the disturbance. The disturbance is coupled to the power supply of the PCB (which represents the Equipment Under Test, briefly EUT) and decoupled from the Power Module (PM, an auxiliary equipment that provides power and control signals to the EUT) through a Coupling/Decoupling Network (CDN).

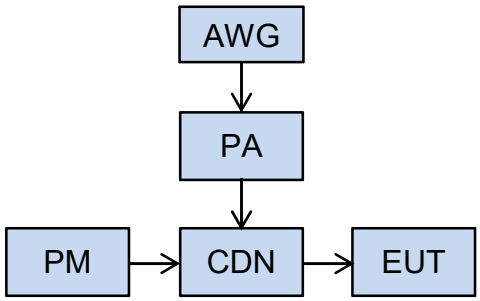

Figure 6. Block diagram representing the experimental setup.

The PA is a current source that injects a high-level current into the bypass network of the PCB. The impedance of the bypass network is very low and ranging from less than one milliohm to few tens of milliohm in the frequency range of interest [11]. This situation corresponds to the one sketched in Figure 4, where the current source is the PA and Z_L is the impedance of the bypass network. The single-ended connection whose transfer impedance significantly impacts on the common mode voltage V_y is the one interested by the flow of the high-level current sourced by the PA, namely the coaxial cable connection from the PA to the CDN, the CDN and the PCB. The common mode voltage V_y at 100 kHz, as measured through an oscilloscope, is shown in Figure 7. The injected current is 10 A and the expected voltage level V_L is about 20 mV, peak-to-peak.

Three situations are considered:

- The RGP is absent and the AWG and the oscilloscope, through which V_y is measured, are commonly referenced to earth through the respective electrical safety conductors. Node y is floating and V_y is large (about 520 mV, peak-to-peak, blue trace in Figure 7) because a large ground loop is formed by the safety conductors and measurement setup that pickups the magnetic field associated to the 100 kHz disturbance.
- The RGP has been introduced in the setup and the AWG and the oscilloscope are connected to the RGP through low impedance bondings. Node y is still floating but V_y has been significantly reduced (210 mV, peak-to-peak, orange trace in Figure 7) due to the reduction of the size of the ground loop.
- Node y is connected to the RGP through a low-impedance binding. A common mode current of about 300 mA (3 % of the injected disturbance current) flows on the RGP, as measured through a current probe clamped around the coaxial cable connecting the PA to the CDN. V_y is further reduced (about 30 mV, peak-to-peak, yellow trace in Figure 7) to a value comparable with the peak-to-peak amplitude of the voltage to be measured, V_L. The CMR offered by the oscilloscope through the two-channels voltage difference is now sufficient to obtain a reliable measurement result of the voltage V_L.

A picture is shown in Figure 8 illustrating the various parts forming the setup [12]. It is not always immediate,

especially when the setup is relatively complex, to identify the origin of an unwanted common mode voltage and the way to reduce its impact on measurement results. The availability of simple models permits to identify the essential features of the problem, to clearly interpret the phenomena and to find appropriate solutions for mitigating unwanted effects.

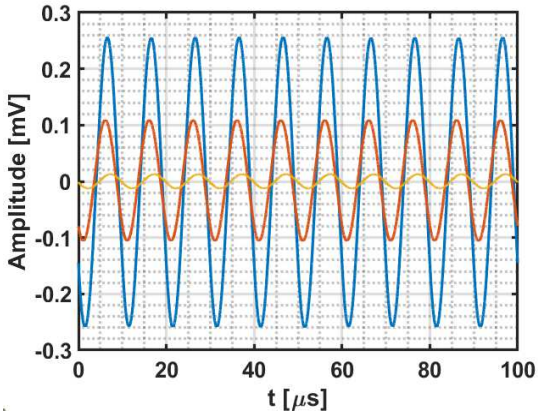

Figure 7. Common mode voltage V_y (see Figure 4) at the disturbance frequency of 100 kHz in the following situations: the AWG and the oscilloscope are connected to earth through the respective safety conductors (blue curve whose peak-to-peak amplitude is about 520 mV), a RGP is introduced and both the AWG and the oscilloscope are connected to the RGP through a low-impedance bonding (red curve whose peak-to-peak amplitude is about 210 mV), also the PCB is connected to the RGP through a low-impedance bonding (orange curve whose peak-to-peak amplitude is about 30 mV).

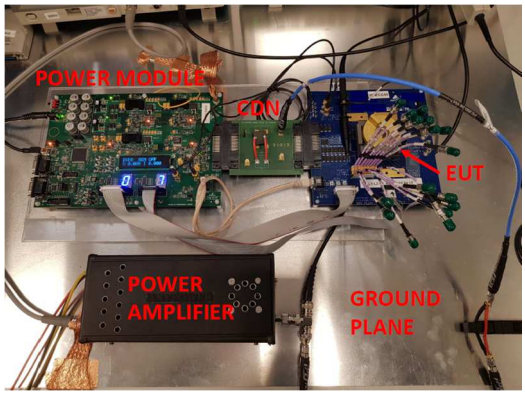

Figure 8. Picture showing the experimental setup. CDN is the Coupling Decoupling Network, EUT is the Equipment Under Test.

References

[1] IEC 62153-4 series: “Metallic communication cables test methods, Electromagnetic compatibility (EMC)”.

[2] C. Carobbi, M. Cati and C. Panconi, "Defining and assessing the uncertainty contributions in the line-injection measurements of transfer impedance," 2008 IEEE International Symposium on Electromagnetic Compatibility, 2008, pp. 1-6, doi: 10.1109/ISEMC.2008.4652097.

[3] J. L. Rotgerink, J. Verpoorte and H. Schippers, "Uncertainties in coaxial cable transfer impedance," in IEEE Electromagnetic Compatibility Magazine, vol. 7, no. 3, pp. 83-93, 3rd Quarter 2018, doi: 10.1109/MEMC.2018.8479344.

[4] C. Tuerk, D. J. Pommerenke and S. Bauer, "Improved Alternative Method for Fast and Simple Transfer Impedance Measurements," in IEEE Letters on Electromagnetic Compatibility Practice and Applications, vol. 2, no. 4, pp. 134-137, Dec. 2020, doi: 10.1109/LEMCPA.2020.3024810.

[5] B. Démoulin, L. Koné, Shielded Cable Transfer Impedance Measurements, IEEE EMC Newsletter, Fall 2010, pp. 30–37.

[6] B. Démoulin, L. Koné, Shielded Cable Transfer Impedance Measurements – High frequency range 100 MHz–1 GHz, IEEE EMC Newsletter, Winter, 2011, pp. 42–50.

[7] B. Démoulin, L. Koné, Shielded Cable Transfer Impedance Measurements in the Microwave Range of 1 GHz to 10 GHz, IEEE EMC Newsletter, Spring, 2011, pp. 52–61.

[8] D. M. Hockanson, J. L. Dreniak, T. H. Hubing, T. P. van Doren, Fei Sha and Cheung-Wei Lam, "Quantifying EMI resulting from finite-impedance reference planes," in IEEE Transactions on Electromagnetic Compatibility, vol. 39, no. 4, pp. 286-297, Nov. 1997, doi: 10.1109/15.649814.

[9] C. F. M. Carobbi, S. Lalléchère and L. R. Arnaut, "Review of Uncertainty Quantification of Measurement and Computational Modeling in EMC Part I: Measurement Uncertainty," in IEEE Transactions on Electromagnetic Compatibility, vol. 61, no. 6, pp. 1690-1698, Dec. 2019, doi: 10.1109/TEMC.2019.2904973.

[10] S. Lalléchère, C. F. M. Carobbi and L. R. Arnaut, "Review of Uncertainty Quantification of Measurement and Computational Modeling in EMC Part II: Computational Uncertainty," in IEEE Transactions on Electromagnetic Compatibility, vol. 61, no. 6, pp. 1699-1706, Dec. 2019, doi: 10.1109/TEMC.2019.2904999.

[11] F. Sordi, L. Capineri and C. Carobbi, "Lumped Circuit Model and VNA Measurement of the RF Impedance of a Bypass Network," 2021 IEEE International Joint EMC/SI/PI and EMC Europe Symposium, 2021, pp. 196-201, doi: 10.1109/EMC/SI/PI/EMCEurope52599.2021.9559217.

[12] Federico Sordi, Leonardo Vignoli, Lorenzo Capineri, and Carlo Carobbi, "Immunity Testing of a SerDes by Power Supply Disturbance Coupling,” submitted to IEEE Transactions on Signal and Power Integrity on Jan. 2022.